Trabajos de Geología, Universidad de Oviedo, 30 : 193-201 (2010)

Oviedo (Spain) 1-3 July 2008 International Meeting of Young Researchers in Structural Geology and Tectonics
YORSGET

3D progressive evolution of a syncline depocentre from growth turbidite strata: the Annot syncline, SE France

L. Salles[1*], M. Ford[2] and P. Joseph[3]

[1]Now at: TOTAL, 2 place J. Millier, La Défense 6, 92400 Courbevoie, France.

[2]Nancy School of Geology, ENSG-CRPG, 15 rue Notre Dame des Pauvres, B.P. 20, 54501 Vandoeuvre-lès-Nancy Cedex, Nancy, France.

[3]Geology-Geochemistry-Geophysics Direction, Institut Français du Pétrole, 228-232 Avenue Napoléon Bonaparte, 92852 Rueil-Malmaison Cedex, France.

[*]e-mail: lise.salles@total.com

Abstract: The Annot syncline is one of the synclinal remnants of the Tertiary Alpine foreland basin, which was mainly structured during the Paleocene and filled during the Eocene-Oligocene by a marine transgressive succession. The upper unit consists in the Annot Sandstone formation deposited in a fan delta-fed turbidite setting. New detailed structural data from the Annot depocentre indicate a progressive limb rotation during deposition of the Annot Sandstone. These data are used to build a 3D model of the syncline in Gocad software that documents turbidite depocentre evolution. Trishear modelling constrains the role and interaction of regional thrusts and fault propagation folds in depocentre development.

Keywords: growth folding, Tertiary alpine foreland basin, limb rotation, migration of depocentre, turbidite, trishear kinematic model.

The Annot Sandstone formation corresponds to the final unit of a marine transgressive succession (named locally the "Nummulitic Trilogy"; Boussac, 1912) of the Alpine foreland basin, preserved in isolated remnants in the fold and thrust belt in SE France (Fig. 1a). The term "depocentre" is used here to describe individual synclinal outliers of the Annot Sandstone (for instance, Annot depocentre, Grand Coyer depocentre, etc) (Fig. 1c). The Annot Sandstone basin corresponds to the foreland basin containing all these depocentres. A considerable volume of key sedimentological and stratigraphical studies have focused on the Annot sand-rich turbidites since the fifties (Stanley, 1961; Bouma 1962; Lanteaume *et al.*, 1967; Ravenne *et al.*, 1987), partly because they are an analogue for oil reservoirs in fan delta-fed turbidite settings. Units within the Annot Sandstone were delimited and mapped in different depocentres (Callec, 2004; Joseph and Lomas, 2004; Puigdefàbregas *et al.*, 2004). More recently, the depositional model of the Annot Sandstone basin was defined as a turbidite submarine ramp fed by multiple-source fan deltas (Pickering and Hilton, 1998; Sinclair, 2000; Joseph *et al.*, 2000). Interconnections of the tectonically active depocentres are found to have been three dimensional and to have evolved over time (Du Fornel *et al.*, 2004). Regional anticlines, which control the Annot Sandstone basin, are considered to be mainly fault

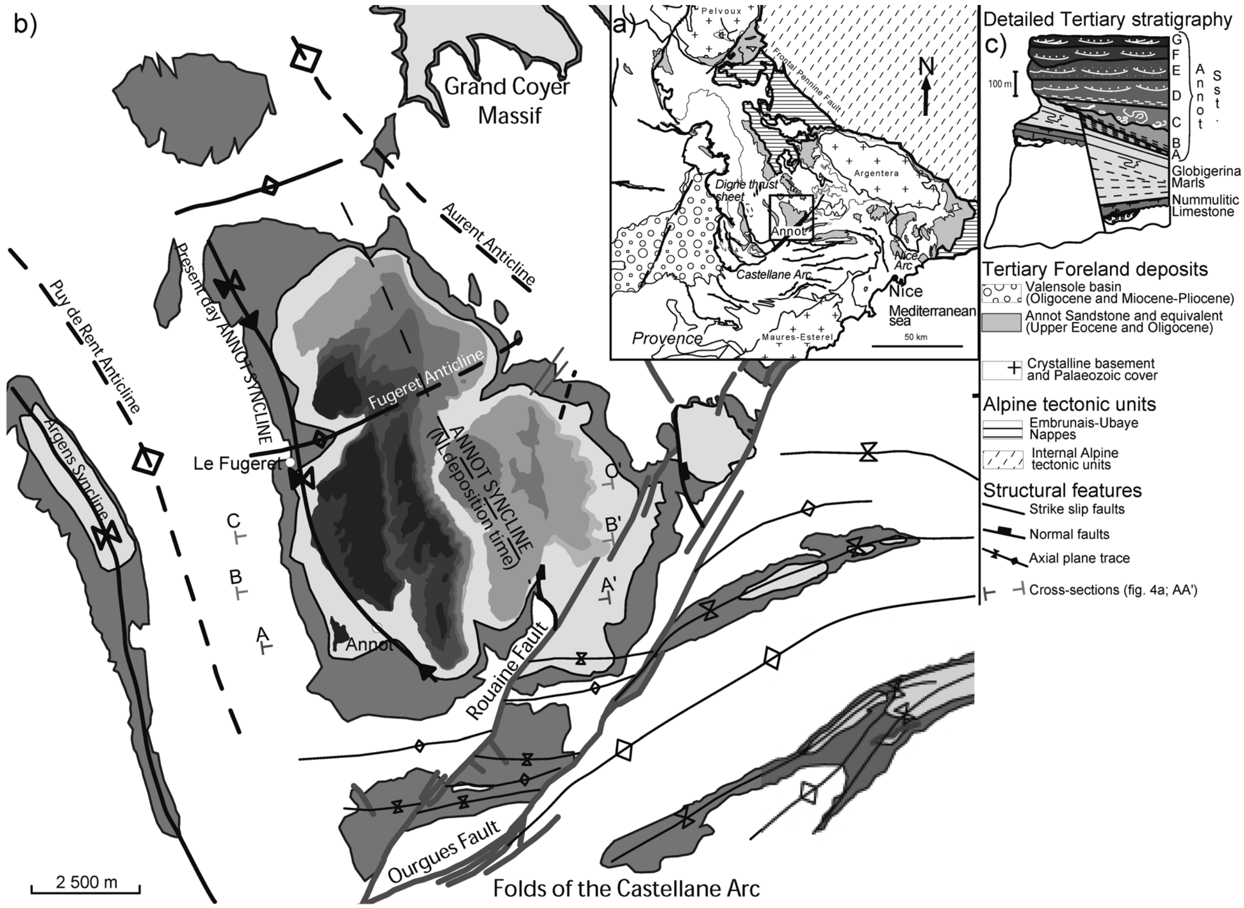

Figure 1. (a) Regional tectonic map of SE France showing the outliers of the alpine foreland basin. The studied area is boxed, (b) Tertiary stratigraphy and structure of the Annot depocentre. Section line A-A' is shown in figure 4a, (c) lithostratigraphy of the Nummulitic Trilogy in the Annot depocentre. Abbreviation: Sst: Sandstone. Syndepositional normal faulting occurs in the Nummulitic Limestone and the Globigerina Marls. Unit B of the Annot Sandstone seals this normal fault. The Annot Sandstone onlaps onto the Globigerina Marls.

propagation folds (Apps, 1987). Nevertheless, precise kinematics and relative dating of the folds remain open questions. Studies of sandstone thickness variations and their controlling structures will constrain the structural framework of the Alpine foreland basin. Furthermore, the turbidites can be used as horizontal paleomarkers and, where they are synchronous with growth folding, their geometries can record fold kinematics. The main objectives of our study are to define the kinematics and relative dating of folds occurring in the Annot depocentre based on deformation recorded by the Annot Sandstone. The approach developed includes detailed structural field analyses and 3D geometrical modelling and trishear kinematic modelling. The studied Annot depocentre covers an area of 70 km² (about 11 km NS by 6 km E-W), at 70 km N-W of Nice (Figs. 1a and 1b). It lies just at the intersection of the Digne thrust sheet (NNW-SSE) and the Castellane arc (E-W) (Fig. 1a). Two fold trends have been observed in the Tertiary sediments: a main NNW-SSE syncline and local E-W folds such as the Fugeret anticline (Apps, 1987; Puigdefàbregas *et al.*, 2004) (Fig. 1b). New detailed structural data collected in the Annot depocentre has been used to build a 3D structural model in Gocad software (Discrete Smooth Interpolation, Mallet, 1989). A thickness map of the Nummulitic Limestone derived from this model shows a synclinal depocentre 5 km east of the present axial trace. From this preliminary result, we decided to examine precisely the geometry and relationship of the Annot Sandstone units to define the processes of folding, in particular depocentre migration and fold limb rotation.

Methods

The Annot depocentre and especially members in the Annot Sandstone have been previously mapped by

Albussaïdi and Laval (1984), Callec (2001) and Puigdefàbregas *et al.* (2004). While these maps are in close agreement for the southern and eastern parts of the Annot depocentre, they differ markedly to the north of the Fugeret anticline. Albussaïdi and Laval's map was found to be the most consistent with our own field observations and, therefore, formed the basis for subsequent mapping of the seven members of the Annot aandstone labelled A to G (Figs. 1b and 1c).

The present study is based on data collected during two field surveys in 2006 and 2007. Over 200 bedding dips were collected in the Annot Sandstone units across the area. These were statistically analysed for each member (Stereonet free software by R. W. Allmendinger).

We drew 3 E-W cross-sections, labelled A-A', B-B', C-C' (Fig. 1b), taking great care to define growth geometries and progressive unconformities. In order to ensure 3D integrity of the interpretation, we built a 3D geometrical model in Gocad software, constrained by dips, outcrop limits and honouring the fault network. Maps of vertical thickness were automatically calculated for each sandstone unit and allow us to study the location and evolution of the depocentre.

Interaction of sedimentation and folding using thickness and dip

We consider three ways in which sedimentation and folding can interact assuming that bedding represents horizontal (Fig. 2): i) passive filling. Successive members infilled an already existing synclinal structure. The fold axis migrated only after deposition, ii) static growth syncline. Successive members filled an active syncline whose axis remained in the same location during deposition and later migrated, and iii) migrating growth syncline. Successive members were deposited in a growth syncline whose axis continuously migrated.

Each of these situations will generate a specific pattern of dip and thickness distribution in growth strata: i) passive filling. Each unit has a constant thickness except in the vicinity of the onlaps. The dip remains the same throughout the whole succession, ii) static growth syncline. The thickness reaches a maximum in

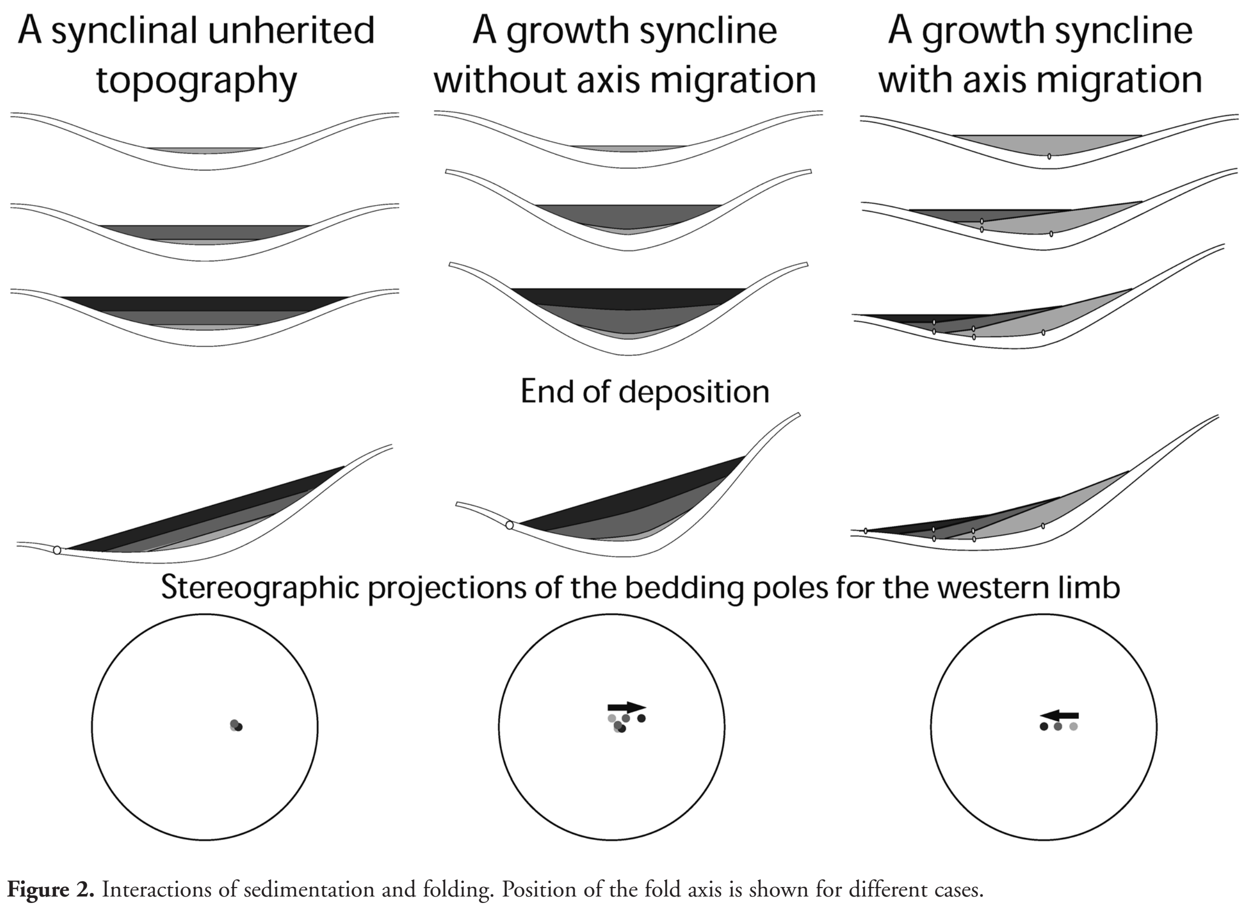

Figure 2. Interactions of sedimentation and folding. Position of the fold axis is shown for different cases.

the axial part of the syncline and decreases toward the limbs. On the left limb, dips in growth strata stay quite constant in a vertical profile but increase from older to younger units in a horizontal section. Here, it is therefore necessary to analyse dip variation along a horizontal profile, and iii) migrating growth syncline. Maximum values of thickness migrate to the left. Dips decrease from older to younger strata in a horizontal and in a vertical section.

Fault propagation fold models

Kink band migration (Suppe, 1983) and limb rotation (for example, trishear; Erslev, 1991; Hardy and Ford, 1997) models are the main fold kinematic models for fault-propagation folds. Models describing fault-propagation folds and also their kinematics in footwall synclines can be derived from the kink-band model (Chester and Chester, 1990; Mitra, 1990; Suppe and Medwedeff, 1990; McNaught and Mitra, 1993). Nonetheless, they assume constant dips and thickness per each limb. The trishear model is therefore found to be more appropriate because of limb rotation and thickness variation. Briefly, the trishear model considers the existence of a ductile deforming triangular area at the tip of a propagating thrust ramp. Slip on the ramp causes a folding in this triangular area. The main parameters of the trishear model are the angle of the triangular zone and the ratio of the propagation rate and the slip rate on the fault. FaultFold_Academy software (Allmendinger, 1998) is freely available on the web and allows the construction of 2D cross-sections honouring kinematic principles of the trishear model.

Analysis/results

Migration of the axis/migration of the depocentre

The main structure of the Annot depocentre is a NNW-SSE-trending syncline (Annot syncline, Fig. 1b), which corresponds to the alpine compression. Nowadays, the axial surface trace is exposed to the west to the outcropping Annot Sandstone (Fig. 1b). However, the westward onlap migration recorded by turbidite deposition and Nummulitic Limestone thickness, derived from our model, suggests a more easterly position for the fold axis. Indeed, thickness variations show active folding during Nummulitic Limestone deposition; the fold axial trace, which corresponds to the line of maximum thickness values, is 5 km east of its present location (Fig. 1b). The axis of the Annot syncline migrated westward. Only the early western limb was preserved and it now lies on the eastern limb of the late syncline. While in the southern part of the depocentre the expression of this fold is evident, the dip pattern in the Annot Sandstone is more complicated further north because of E-W structures. We chose to distinguish two areas delimited by the southern limit of influence of this Fugeret structure (Fig. 1b). In order to propose kinematics of the Annot syncline, only the dips in the southern part are considered. The geometry of Fugeret fold (Fig. 1b) and its interaction with the Annot syncline (Fig. 1b) are then described using other dips.

Dip pattern for the Annot syncline

On the stereographic projections of bedding poles (Stereonet software, figures 3a and 3b), plunge increases from unit A to unit D. For the upper units (E, F and G), poles are globally in the same position. It appears, however, that the poles of unit F plunge more than those of unit E. In this case, the scatter of data may be relative to measurement errors. By comparing with the models for interaction of sedimentation and folding presented before (Fig. 2), these results illustrate a migration of the fold axis during deposition of sandstone units A to D (case of the migrating growth syncline). Thus, the folding seems to be less active during deposition of units D to G.

Thickness pattern for the Annot syncline

The models, presented in figure 2, show that thickness distribution can also provide information to define the interaction between sedimentation and folding. One of our three E-W cross-sections (A-A') is presented in figure 4a. Its transect (Fig. 1b) cuts through two famous and spectacular outcrops of the Annot depocentre (Braux road cut and Chambre du Roi cliff). A progressive westward migration of maximum thickness values is documented. The results for the two other cross-sections are similar. The structural analysis in 2D reveals a migrating growth syncline. Regarding the progressive evolution of the depocentre, information provided by the 3D model, is in agreement with a progressive westward migration for the units labelled from C to G. Indeed, vertical thickness maps of units D and F (Figs. 4c and 4d) show a submeridian zone of maximum values. From unit D to unit F, this depocentre has migrated about 2.5 km westward. For the lower units, thickness pattern is more complex. For instance, unit B presents larger variations; it is less than 50 m thick on the Fugeret anticline and reaches up 330 m just to the north of this structure (Fig. 4b). A NNE-SSW minimum thickness zone is observed above the Braux normal fault (Figs. 1b and 4b). Even if the base of unit B

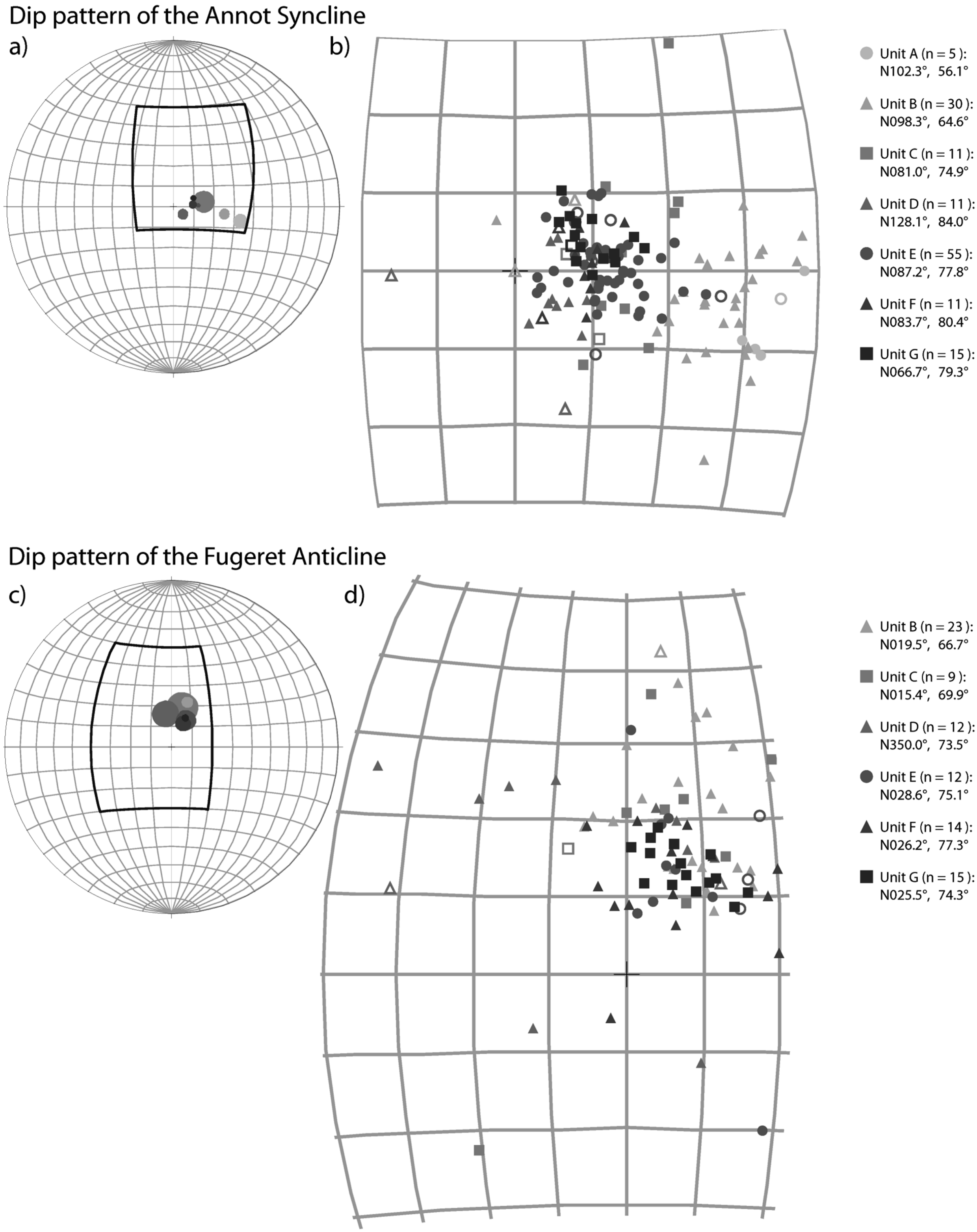

Figure 3. Stereographic projections. (a) Mean vectors of the bedding poles and (b) bedding poles of the Annot syncline, (c) mean vectors of the bedding poles and (d) bedding poles of the Fugeret anticline. Open symbols have a higher uncertainty.

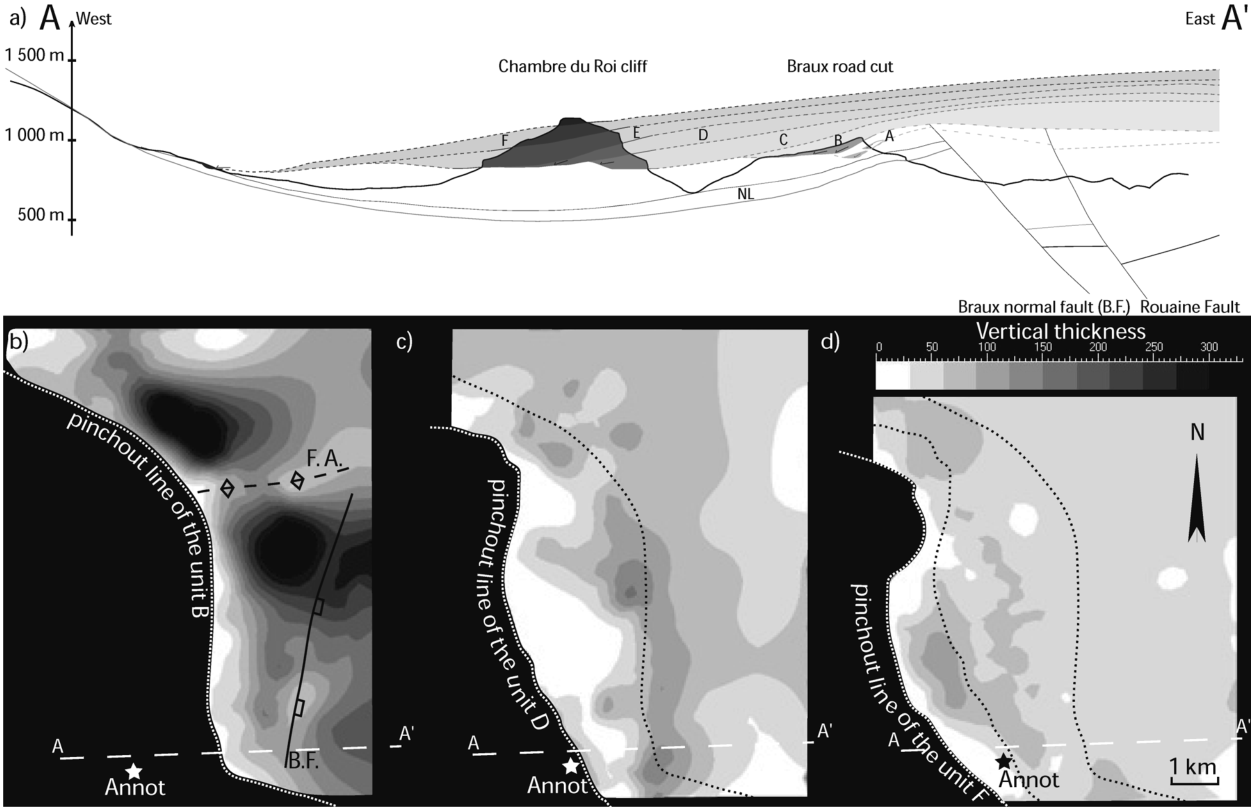

Figure 4. (a) E-W section line A-A' across the Annot depocentre. See figure 1b for location. NL: Nummulitic Limestone. (b-c-d). Vertical thickness maps for units B, D and F respectively. These maps are derived from 3D modelling in Gocad. Section line A-A' just above is located on the maps. While thickness clearly indicates a NNW-SSE trough for the upper two units, thickness variations in unit B are more complex. Deposition of this unit has interacted with the Fugeret anticline (F.A.) and the Braux normal fault (B.F.).

seals the fault (Fig. 1c), it seems that the hanging wall zone close to the fault was slightly higher at the beginning of deposition of unit B. Concerning the Fugeret anticline, we tried to date its development relative to the NNW-SSE syncline and study their possible interferences. The poles of bedding relative to the Fugeret structure were plotted on a Schmidt canvas (Figs. 3c and 3d). The poles of the units from C to G scatter at the same location. The Fugeret structure was therefore largely inactive during the turbidite deposition. This result is in agreement with vertical thickness maps of the upper units, derived from the 3D model, where no significant thickness variation is observed in the vicinity of the Fugeret anticline (Figs. 4c and 4d).

Discussion

Comparison with kinematic models of fault-propagation folds

The analysis of field data indicates two specific processes for folding at Annot: limb rotation and migration of the fold axis. The kink-band migration kinematic model (Suppe and Medwedeff, 1990) has difficulty in reproducing these observations. However, more recently, Scharer *et al.* (2006) propose that a limb rotation on a detachment-fold can be explained by a derivative of this model. Limb rotation can be explained by the trishear model. Ford *et al.*, (1997) also demonstrate hinge line migration and that the hinge line can be discontinuous in the case of erosion. Nevertheless, the migration is directed toward the anticline and not the basin as observed at Annot. We made preliminary tests using the trishear model (FaultFold_Academy software by Allmendinger, 1998) in order to ascertain whether a foreland migration may be possible. Figure 5 shows the simplest configuration for which a migration toward the basin can be reproduced. But if this result is carefully analysed, it is actually the depocentre and not the fold axis which migrates. Trough point is defined as the lowest point of a folded surface and so the depocentre always corresponds to this point. While the trough point and synclinal hinge point are merged in symmetrical fold, the trough point is toward the foreland from the synclinal hinge point in an asymmetrical fold. In studies of monoclinal folds, which are an end-member of an asymmetrical fold, authors have already distinguished the depocentre from the hinge zone (Poblet *et al.*, 2004).

Relative dating of the structures recorded by the Annot Sandstone formation

From the dip pattern analysed above, we can propose a relative timing of the structures. Two principal trends are expressed in the Annot depocentre. The main one (NNW-SSE) includes the Annot syncline and its two adjacent anticlines (Puy de Rent and Aurent-Mélina, figure 1b) and is clearly linked with the Alpine orogenesis (Apps, 1987). The Fugeret anticline (Fig. 1b) is the only E-W fold preserved within the Annot Sandstone. There also exists an E-W high zone which separates the Annot and the Grand Coyer depocentres, suggesting the existence of a northern closure of the turbidite basin. The timing of the Fugeret anticline may indicate an age for this parallel structure.

The westward onlap characteristics in the Annot Sandstone indicate that the western anticline, Puy de Rent anticline (Fig. 1b), was already a significant feature before sandstone deposition. Our study shows, furthermore, that sedimentation was controlled by the growth of the eastern anticline, the Aurent-Mélina anticline (Fig. 1b), which led to the progressive tilting of the eastern limb of the Annot syncline. The simultaneous development of both anticlines may be due to the presence of a salt detachment (Costa and Vendeville, 2002) in the Triassic deposits. In the westernmost Sandstone outcrops, Albussaïdi and Laval (1984) noted an onlap in the uppermost unit and measured a horizontal dip. These observations date the synchronous end of folding and of turbidite deposition in the Annot depocentre.

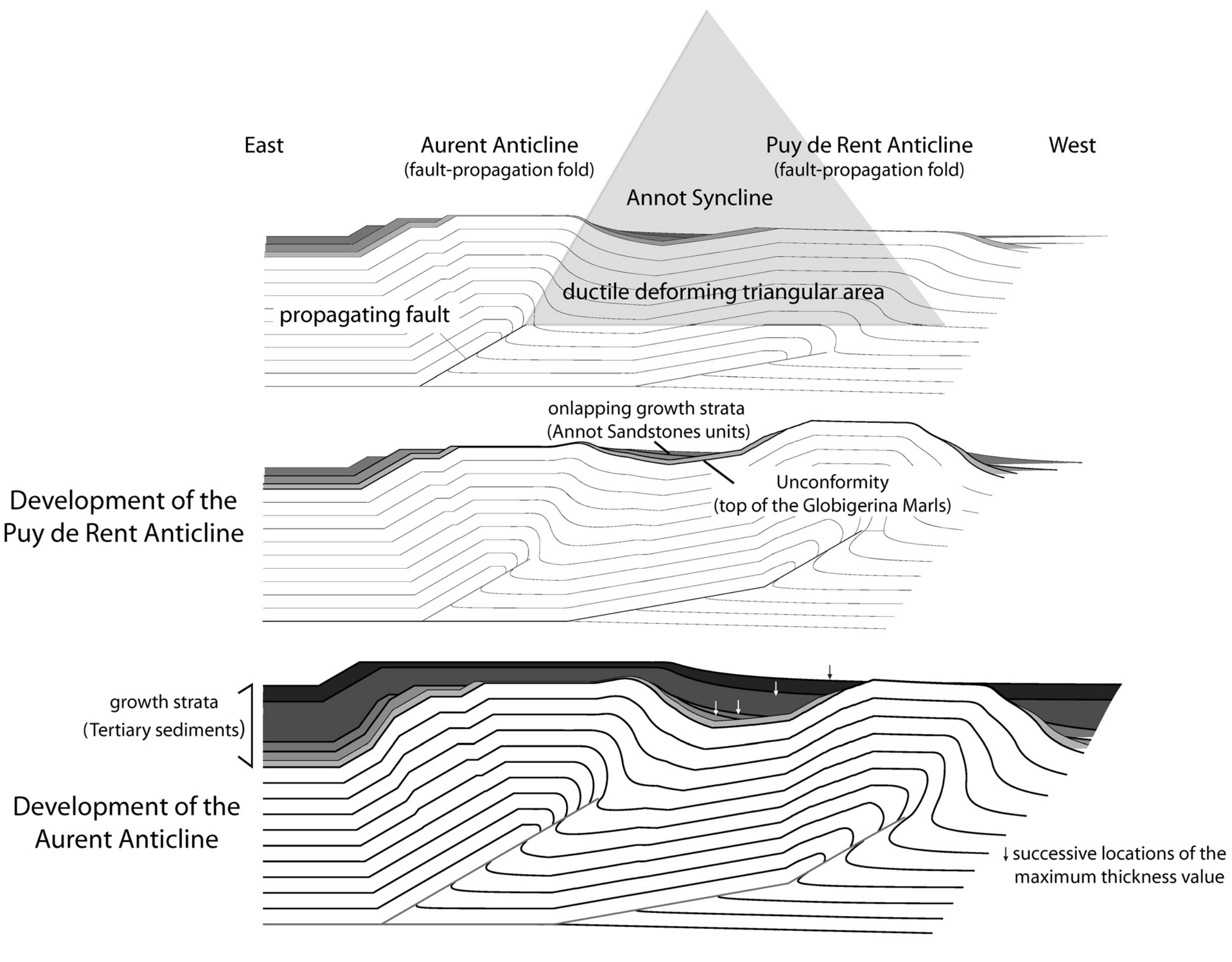

Figure 5. Preliminary test with trishear kinematic model showing a limb rotation and a depocentre migration within the growth strata (coloured in grey). The cross-section is made using the FaultFold_Academy. It is not scaled on the precise case of the Annot depocentre.

Since the study of Apps (1987), the presence of a paleorelief between the Annot and Grand Coyer depocentres and the northern implied closure of the Annot depocentre has been an open question. Based on detailed analysis of the Fugeret structure, we can propose new insight. Firstly, Albussaïdi and Laval (1984) observed that units B to D lie directly on the Globigerina Marls just to the north of the Fugeret anticline and that onlap offsets southward up through the whole Annot Sandstone sequence. An E-W Fugeret anticline therefore existed before Sandstone deposition and perhaps before deposition of the Nummulitic Limestone and the Globigerina Marls. However, we measured only one low northward dip while implying a later southward tilting. Secondly, dip analysis within the Annot Sandstone presented above (Fig. 3c) indicates activity only during deposition of unit B. We therefore propose an early Alpine reactivation of older E-W structures (perhaps linked with the Pyrenean-Provencal orogenesis) which ended at the beginning of Annot Sandstone deposition. Later southward tilting could be linked with the Miocene N-S compression event in the Castellane arc, just to the south of Annot (Laurent *et al.*, 2000).

Conclusions

Our study demonstrates that WSW-verging folds controlled the Annot Sandstone deposition. In particular, the development of the Aurent-Mélina anticline (Fig. 1b), which corresponds to a fault-propagation fold just to the east of the Annot syncline, induced a progressive limb rotation and a depocentre migration. Thickness variation and dip pattern within the Annot Sandstone are proof of this interaction between tectonics and sedimentation. An approach between structural field work and kinematic modelling addresses the issue of structure at depth. NNW-SSE fault-propagation folds detached on a Triassic salt level can explain the turbidite deposition pattern observed in the Annot syncline. Existence of E-W folds advocates the use of 3D surface modelling to explore their possible interaction with NNW-SSE folds and date the structures. Thickness maps, derived from our field-data based 3D model, indicates structures interacting with deposition. The lower part of the Annot Sandstone sequence (units A and B) remained essentially controlled by the Braux normal fault, which was mainly active during sedimentation of the Nummulitic Limestone and the Globigerina Marls, and the Fugeret anticline. Maps of the upper units illustrate a significant influence of the NNW-SSE growth syncline and demonstrate a westward depocentre migration. Similar studies of structural controls on turbidite deposition are being carried out in other depocentres of the Annot Sandstone basin (especially in the Sanguinière and the Tête de Méric depocentres).

Acknowledgements

Lise Salles PhD study is funded by TOTAL and an ANR project led by Antoine Le Solleuz.

References

ALBUSSAÏDI, S. and LAVAL, A. (1984): *Nouvelles observations de la série Priabonienne. Evolution latérale en relation avec la tectonique.* Diplôme ENSPM, ref 32677, Ecole Nationale Supérieure du Pétrole et des Moteurs, Institut Français du Pétrole, Rueil-Malmaison, 86 pp.

ALLMENDINGER, R. W. (1998): Inverse and forward numerical modeling of trishear fault-propagation folds. *Tectonics*, 17: 640-656.

APPS, G. (1987): *Evolution of the Grès d'Annot basin, SW Alps.* Unpublished PhD Thesis, University of Liverpool, 352 pp.

BOUMA, A. H. (1962): *Sedimentology of some flysch deposits: a graphic approach to facies interpretation*. Elsevier Pub. Co., 159 pp.

BOUSSAC, J. (1912): *Etudes stratigraphiques sur le Nummulitique alpin*. *Mém. Carte Géol. Fr.*, 662 pp.

CALLEC, Y. (2001): *La déformation synsédimentaire des bassins paléogènes de l'arc de Castellane (Annot, Barrême, Saint Antonin).* PhD Thesis, Ecole des Mines de Paris, Paris, 674 pp.

CALLEC, Y. (2004): The turbidite fill of the Annot sub-basin (SE France): a sequence-stratigraphy approach. In: P. JOSEPH and S. A. LOMAS (eds): *Deep-Water sedimentation in the Alpine Basin of SE France: new perspectives on the Grès d'Annot and related systems. Geol. Soc. London Spec. Publ.*, 221: 111-135.

CHESTER, J. S. and CHESTER, F. M. (1990): Fault-propagation folds above thrusts with constant dip. *J. Struct. Geol.*, 12: 903-910.

COSTA, E. and VENDEVILLE, B. (2002): Experimental insights on the geometry and kinematics of fold-and-thrust belts above weak, viscous evaporitic décollement. *J. Struct. Geol.*, 24: 1729-1739.

DU FORNEL, E., JOSEPH, P., DESAUBLIAUX, G., ESCHARD, R., GUILLOCHEAU, F., LERAT, O., MULLER, C., RAVENNE, C. and SZTRÀKOS, K. (2004): The southern Grès d'Annot outcrops (French Alps): an attempt at regional correlation. In: P. JOSEPH and S. A. LOMAS (eds): *Deep-Water sedimentation in the Alpine Basin of SE France: new perspectives on the Grès d'Annot and related systems. Geol. Soc. London Spec. Publ.*, 221: 137-160.

ERSLEV, E. A. (1991): Trishear fault-propagation folding. *Geology*, 19: 617-620.

FORD, M., WILLIAMS, E. A., ARTONI, A., VERGÉS, J. and HARDY, S. (1997): Progressive evolution of a fault-related fold pair from growth strata geometries, Sant Llorenç de Morunys, SE Pyrenees. *J. Struct. Geol.*, 19: 413-441.

HARDY, S. and FORD, M. (1997): Numerical modeling of trishear fault propagation folding. *Tectonics*, 16: 841-854.

JOSEPH, P., BABONNEAU, N., BOURGEOIS, A., COTTERET, G., ESCHARD, R., GARIN, B., GOMES DE SOUZA, O., GRANJEON, D., GUILLOCHEAU, F., LERAT, O., QUEMENER, J. M. and RAVENNE, C. (2000): The Annot Sandstone outcrops (French Alps): architecture description as input for quantification and 3D reservoir modeling. In: P. WEIMER, R. M. SLATT, J. COLEMAN, N. C. ROSEN, H. NELSON, A. H. BOUMA, M. J. STYZEN and D. T. LAWRENCE (eds): *Deep-Water Reservoirs of the World, SEPM (CD-ROM) Spec. Publ.*, 28: 422-449.

JOSEPH, P. and LOMAS, S. A. (2004): Deep-Water Sedimentation in the Alpine Foreland Basin of SE France: New perspectives on the Grès d'Annot and related systems – an introduction. In: P. JOSEPH and S. A. LOMAS (eds): *Deep-Water sedimentation in the Alpine Basin of SE France: new perspectives on the Grès d'Annot and related systems. Geol. Soc. London Spec. Publ.*, 221: 1-16.

LANTEAUME, M., BEAUDOIN, B. and CAMPREDON, R. (1967): *Figures sédimentaires du flysh "Grès d'Annot", synclinal de Peïra-Cava*. Edition du Centre National de la Recherche Scientifique, 99 pp.

LAURENT, O., STEPHAN, J. F. and POPOFF, M. (2000): Modalité de la structuration miocène de la branche sud de l'arc de Castellane (chaînes subalpines méridionales). *Géol. Fr.*, 3: 33-65.

MALLET, J. L. (1989): Discrete smooth interpolation. *ACM T. Graphic.*, 8: 121-144.

MCNAUGHT, M. A. and MITRA, G. (1993): A kinematic model for the origin of footwall synclines. *J. Struct. Geol.*, 15: 805-808.

MITRA, S. (1990): Fault-Propagation Folds: Geometry, Kinematic Evolution, and Hydrocarbon Traps. *AAPG Bull.*, 74: 921-945.

PICKERING, K. T. and HILTON, V. C. (1998): *Turbidite systems of Southeast France*. Vallis Press, London, 229 pp.

POBLET, J., BULNES, M., MCCLAY, K. and HARDY, S. (2004): Plots of Crestal Structural Relief and Fold Area versus Shortening – A Graphical Technique to Unravel the Kinematics of Thrust-related Folds. In: K. R. MCCLAY (ed): *Thrust tectonics and hydrocarbon systems, AAPG Mem.*, 82: 372-399.

PUIGDEFÀBREGAS, C., GJELBERG, J. and VAKSDAL, M. (2004): The Grès d'Annot in the Annot syncline: outer basin-margin onlap and associated soft-sediment deformation. In: P. JOSEPH and S. A. LOMAS (eds): *Deep-Water sedimentation in the Alpine Basin of SE France: new perspectives on the Grès d'Annot and related systems. Geol. Soc. London Spec. Publ.*, 221: 367-388.

RAVENNE, C., VIALLY, R., RICHÉ, P. and TRÉMOLIÈRES, P. (1987): Sédimentation et tectonique dans le bassin marin Eocène supérieur-Oligocène des Alpes du Sud. *Rev. I. Fr. Petrol.*, 42: 529-553.

SCHARER, K. M., BURBANK, D. W., CHEN, J. and WELDON II, R. J. (2006): Kinematic models of fluvial terraces over active detachment folds: Constraints on the growth mechanism of the Kashi-Atushi fold system, Chinese Tian Shan. *Geol. Soc. Am. Bull.*, 118: 1006-1021.

SINCLAIR, H. D. (2000): Delta-fed turbidites infilling topographically complex basins: a new depositional model for the Annot Sandstones, SE France. *J. Sediment. Res.*, 70: 504-519.

STANLEY, D. J. (1961): Etudes sédimentologiques des Grès d'Annot et de leurs équivalents latéraux. *Rev. I. Fr. Petrol.*, 16, 11: 1231-1254.

SUPPE, J. (1983): Geometry and kinematics of fault-bend folding. *Am. J. Sci.*, 283: 684-721.

SUPPE, J. and MEDWEDEFF, D. A. (1990): Geometry and kinematics of fault-propagation folding. *Eclogae Geol. Helv.*, 83: 409-454.